Molecular Design by Cycloaddition Reactions. 37.[1] Peri-, Stereo-, and Regioselectivities in Cycloaddition Reactions of 7-Isopropylidenebenzonorbornadiene

Tadashi Sasaki,* Kenji Hayakawa, Takashi Manabe, and Sumio Nishida

Contribution from the Institute of Applied Organic Chemistry, Faculty of Engineering, Nagoya University, Furo-cho, Chikusa-ku, Nagoya 464, Japan. *Received April 1, 1980*

Abstract: Cycloaddition reactions of the titled compound **1** with dienes, 1,3-dipoles, and heterocumulenes have been investigated in order to study the origin of its peri-, stereo-, and regioselectivities. Both dienes **4–6** and 1,3-dipoles **12–15** reacted with **1** to give Diels–Alder adducts **7–9** and 1,3-dipolar cycloadducts **16–19**, respectively, in good yields. In these reactions, **1** reacted only at the endocyclic double bond and the exocyclic double bond remained unchanged. In contrast, **1** reacted with dichloroketone at both its endocyclic and exocyclic double bonds to give **20** (27%) and *anti*-**21** (18%), *syn*-**22** (13%), respectively. The similar but increased stereoselectivity was observed in the similar reaction of dihydro compound **2**, and two adducts *anti*-**28** (40%) and *syn*-**29** (13%) were obtained. The reaction of **1** with chlorosulfonyl isocyanate (CSI) took place in a stereospecific fashion to give the syn adduct **30a** (69%) which was converted to the β-lactam **30b** (95%) and dihydro derivative **31** (72%) by succesive dechlorosulfonylation and catalytic hydrogenation. The stereoselectivity was dramatically changed in the similar reaction of **2**, which after dechlorosulfonylation gave adducts **34** (90%) and **35** (6.8%). The structures of adducts were determined on the basis of spectroscopic data, chemical conversions, and X-ray diffraction analyses.

From the viewpoint of synthetic usefulness and theoretical interest, 7-isopropylidenebenzonorbornadiene (**1**) and its derivatives

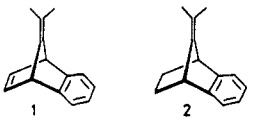

have received considerable attention in the past few years.[2-21] The unique electronic structure is known to affect their chemical reactivities. The energetic proximity of its highest occupied (HOMO) and lowest unoccupied molecular orbitals (LUMO) enables **1** to perform both HOMO-controlled and LUMO-controlled reactions,[22,23] depending on the situation. In the Diels–Alder reaction, **1** showed as a dienophile a significant rate increase as compared with benzonorbornadiene for additions with "inverse electron demand" (i.e., HOMO(**1**) controlled), while almost no rate enhancement was observed for "normal" addition (i.e., LUMO(**1**) controlled).[11,12] This remarkable effect of the nonreacting exocyclic double bond was reasonably explained on the basis of the shape and the energy of the frontier orbitals. In contrast, electrophilic additions proceeding through polarized transition states take place only at the exocyclic double bond.[19,24] Recently, Mukai[25,26] and Paquette[27] have independently reported

Table I. Reactions of 7-Isopropylidenebenzonorbornadiene **1** with Some Dienes and 1,3-Dipolar Compounds

Addend	Condition employed	Product[a]	Yield[b]
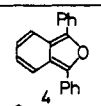 **4**	C_6H_6, 70-80°[c], 160 h.	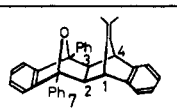	95%
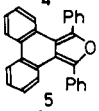 **5**	C_6H_5Cl, 110-120°[c], 120 h.	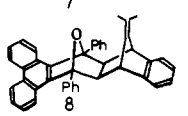 **8**	82%
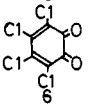 **6**	C_6H_6, 70-80°[c], 20 h.	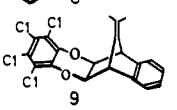 **9**	18%
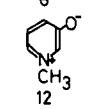 **12**	$C_6H_5CH_3$, reflux, 10 h.	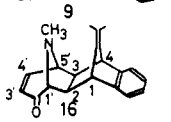 **16**	10%
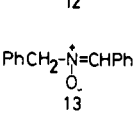 **13**	$C_6H_5CH_3$, reflux, 15 h.	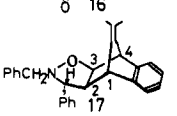 **17**	75%
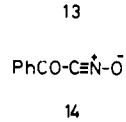 **14**	$(C_2H_5)_2O$, room. temp., 1 day	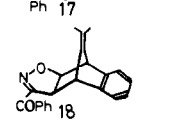 **18**	90%
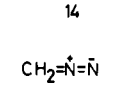 **15**	$(C_2H_5)_2O$, room. temp., 1 day	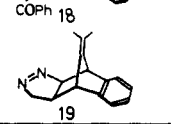 **19**	80%

[a] Numbering shown in the figures is arbitrary. [b] Isolated yields. [c] In a sealed tube.

(1) Part 36 of this series: Sasaki, T.; Manabe, T.; Wakabayashi, E. *Tetrahedron.*, in press.
(2) Muneyuki, R.; Tanida, H. *J. Org. Chem.* **1966**, *31*, 1988.
(3) Tanida, H.; Irie, T.; Tori, K. *Bull. Chem. Soc. Jpn.* **1972**, *45*, 1999.
(4) Watoson, P. L.; Warrener, R. N. *Aust. J. Chem.* **1973**, *26*, 1725.
(5) Lombardo, L.; Wege, D.; Wilkinson, S. P. *Aust. J. Chem.* **1974**, *27*, 143.
(6) Sasaki, T.; Kanematsu, K.; Iizuka, K. *J. Chem. Soc., Perkin Trans. 1* **1974**, 933.
(7) Sasaki, T.; Kanematsu, K.; Iizuka, K. *Tetrahedron* **1975**, *31*, 1671.
(8) Warrener, R. N.; Paddon-Row, M. N. *Tetrahedron Lett.* **1977**, 3291.
(9) Goldstein, M. J.; Hoffmann, R. *J. Am. Chem. Soc.* **1971**, *93*, 6193.
(10) Inagaki, S.; Fujimoto, H.; Fukui, K. *J. Am. Chem. Soc.* **1976**, *98*, 4693.
(11) Haselbach, E.; Rossi, M. *Helv. Chim. Acta* **1976**, *59*, 278.
(12) Pfaendler, H. R.; Tanida, H.; Haselbach, E. *Helv. Chim. Acta* **1974**, *57*, 383.
(13) Tori, K.; Ueyama, M.; Tsuji, T.; Matsumura, H.; Tanida, H.; Iwamura, H. *Tetrahedron Lett.* **1974**, 327.
(14) Knothe, L.; Werp, J.; Babsch, H.; Prinzbach, H.; Fritz, H. *Justus Liebigs Ann. Chem.* **1977**, 709.
(15) Brogli, F.; Giovannini, E.; Heilbronner, E.; Schuster, R. *Chem. Ber.* **1973**, *106*, 961.
(16) Heilbronner, E.; Martin, H. D. *Helv. Chim. Acta* **1972**, *55*, 1490.
(17) Bingham, R. C.; Dewar, M. J. S.; Lo, D. H. *J. Am. Chem. Soc.* **1975**, *97*, 1285.
(18) Hoffmann, R. W.; Schuttler, R.; Schafer, W.; Schweig, A. *Angew. Chem., Int. Ed. Engl.* **1972**, *11*, 512.
(19) Paquette, L. A.; Broadhurst, M. J. *J. Org. Chem.* **1973**, *38*, 1893.
(20) Hoffmann, R. W.; Kurz, H. *Chem. Ber.* **1975**, *108*, 119.
(21) Paquette, L. A.; Oku, M.; Farnham, W. B.; Olah, G. A.; Liang, G. *J. Org. Chem.* **1975**, *40*, 700.
(22) Houk, K. N.; Sims, J.; Watts, C. R.; Luskus, L. J. *J. Am. Chem. Soc.* **1973**, *95*, 7301.
(23) Sustmann, R. *Tetrahedron Lett.* **1971**, 2717, 2721.
(24) Hertel, L. W.; Paquette, L. A. *J. Am. Chem. Soc.* **1979**, *101*, 7620.

0002-7863/81/1503-565$01.00/0

stereoselective addition of singlet oxygen to 7-isopropylidenebenzonorbornene (**2**) and related systems and have concluded that the π-orbital distortion of the exocyclic double bond is one of the most important factors controlling the stereoselectivity.

Despite considerable work on **1**, no explanation for the periselectivity[28] in cycloaddition of **1** has been made so far. As part of our systematic studies on the reactivity of 7-substituted benzonorbornadienes,[6,29,30] we have investigated the cycloaddition reactions of **1** with various dienes, 1,3-dipoles, and heterocumulenes. It was found that dichloroketene reacted with both exocyclic and endocyclic double bonds of **1**, while the Diels–Alder reaction and the 1,3-dipolar cycloaddition took place exclusively on the endocyclic double bond. In contrast, chlorosulfonyl isocyanate (CSI) attacked only the exocyclic double bond. These results provide valuable information concerning the nature of periselectivity of **1**. Furthermore, stereoselectivity and regiospecificity of heterocumulene addition to the exocyclic double bond of **1** and **2** are also studied, and the important factors controlling them are discussed.

Results

Reactions of 1 with Dienes. Diels–Alder reaction of **1** has been investigated mostly in the course of the preparation of transient 8,8-dimethylisobenzofulvene.[3,4] Recently, we[6] and Pfaendler et al.[12] independently found that **1** also reacted smoothly with electron-deficient tropone to give the exo,endo adduct **3** in a good yield.

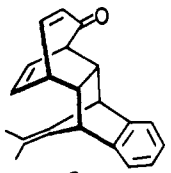

3

Reactions with other cyclic dienes were studied and the results are summarized in Table I. 1,3-Diphenylisobenzofuran (**4**) and its benzologue **5** were allowed to react with **1** to give 1:1 adducts **7** and **8** in 95% and 82% yields, respectively. The structural proof was based on elemental analyses and spectroscopic data. The mass spectrum of **7** exhibited a parent ion peak at *m/e* 452 and a characteristic fragment peak at *m/e* 270 (1,3-diphenylisobenzofuran). The symmetric structure is evident in its ^{1}H NMR spectrum showing signals at δ 1.21 (s, 6 H, $CH_3 \times 2$), 2.53 (s, 2 H, H-2 and H-3), 3.49 (s, 2 H, H-1 and H-4), and 6.8–7.8 (m, 18 H, aromatic H). The absence of vicinal couplings ($J_{1,2}$ and $J_{3,4}$) indicated the bridgehead protons (H-2 and H-3) to be endo to the 7-isopropylidenebenzonorbornadiene system. The exo,endo configuration (e.g., **10**) was ruled out by the rather "normal" chemical shift of the isopropylidene methyl groups (**7**, 1.21; **8**, 0.93 ppm), because the abnormally strong high-field shift of these signals (0.17 ppm) was observed in the related exo,endo adduct **11**[31] due to the anisotropic effect of the proximate aromatic ring. Thus, the adducts **7** and **8** were assigned as exo,endo [4 + 2] (or [8 + 2]) cycloadducts.

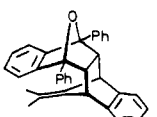

10

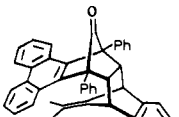

11

Scheme I

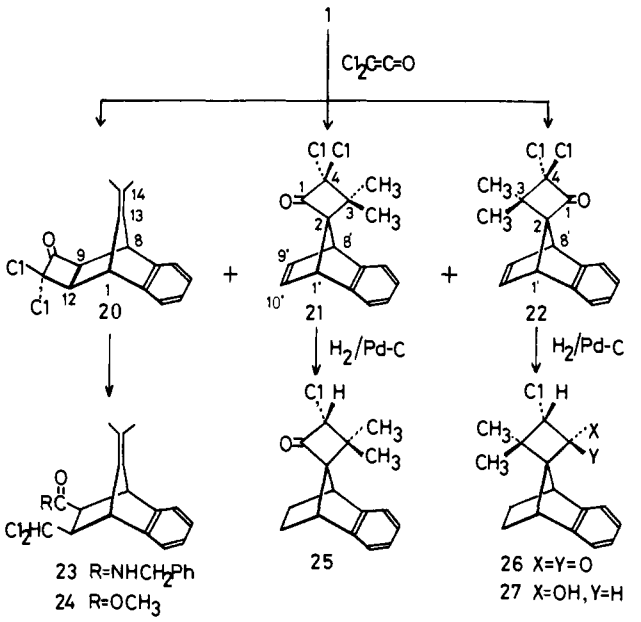

Reaction of **1** with *o*-chloranil (**6**) afforded 1:1 adduct **9** in low yield. The IR spectrum showed no carbonyl bands and the ^{1}H NMR spectrum revealed the absence of couplings between H-1 and H-2 (H-3 and H-4). Thus, **9** was assigned to be the C–O-bonded [4 + 2] (or [8 + 2]) cycloadduct with exo configuration. The preferred bond formation at carbonyl oxygen atoms can be attributed to the steric hindrance of the bridged isopropylidene group. This is a sharp contrast to the reported results of the reaction of **6** and norbornadiene, which gave the C–C-bonded [4 + 2] adduct as the major product.[32] 6,6-Dimethyl- and 6,6-diphenylfulvene and furan were found to be inert in the reaction with **1**.

Reactions of 1 with 1,3-Dipoles. It is rather surprising that no reports on 1,3-dipolar cycloaddition of **1** have been published. The high reactivity of **1** as a dipolarophile is now shown by the following experimental results (Table I). Reaction of **1** with 1-methylpyridinium-3-olate (**12**) afforded 1:1 adduct **16** in 10% yield. The IR spectrum exhibited an α,β-unsaturated carbonyl band at 1660 cm^{-1}. In the ^{1}H NMR spectrum (Experimental Section), the absence of vicinal couplings bewteen H-1′ and H-2 (H-3 and H-5′) and between H-1 and H-2 (H-3 and H-4) indicated the exo,exo configuration of **16**.

Compound **1** reacted also with *C*-phenyl-*N*-benzylnitrone (**13**), phenylglyoxylonitril oxide (**14**), and diazomethane (**15**) to give 1:1 adducts **17**, **18**, and **19**, respectively, in high yields. The exo configurations of these adducts were confirmed by the ^{1}H NMR spectra ($J_{1,2} = J_{3,4} = 0$). The trans geometry of benzylic methine proton to H-2 in **17** was determined on the basis of its coupling constant (J = 7.2 Hz).[33] The reaction of **1** with benzenesulfonyl azide and tosyl azide gave rise to a complex mixture, while similar reaction with 1-adamantyl azide afforded 1:1 adduct in good yield.[34]

All the reactions observed thus far took place only at the endocyclic double bond of **1**, and the exocyclic double bond remained unchanged.

Reaction of 1 with Dichloroketene. Among the several known methods for preparing unstable dichloroketene, we used here an improved procedure recently reported by Krepski and Hassner.[35] Thus, dichloroketene which was generated in situ by dehalogenation of trichloroacetyl chloride with activated zinc in the presence

(25) Okada, K.; Mukai, T. *J. Am. Chem. Soc.* **1978**, *100*, 6509.
(26) Okada, K.; Mukai, T. *Tetrahedron Lett.* **1979**, 3429.
(27) Paquette, L. A.; Hertel, L. W.; Gleiter, R.; Böhm, M. *J. Am. Chem. Soc.* **1978**, *100*, 6510.
(28) Houk, K. N.; Luskus, L. J.; Bhacca, N. S. *J. Am. Chem. Soc.* **1970**, *92*, 6392.
(29) Sasaki, T.; Kanematsu, K.; Hayakawa, K.; Kondo, A. *J. Org. Chem.* **1973**, *38*, 4100.
(30) Sasaki, T.; Manabe, T.; Nishida, S. *J. Org. Chem.* **1980**, *45*, 476, 479.
(31) Sasaki, T.; Kanematsu, K.; Iizuka, K. *J. Org. Chem.* **1976**, *41*, 1105.
(32) Warrener, R. N.; Nunn, E. E.; Wilson, W. S. *Tetrahedron Lett.* **1972**, 175.
(33) Huisgen, R.; Grashey, R.; Hauck, H.; Seidl, H. *Chem. Ber.* **1968**, *101*, 2043.
(34) Sasaki, T.; Eguchi, S.; Yamaguchi, M., unpublished results.
(35) Krepski, L. R.; Hassner, A. *J. Org. Chem.* **1978**, *43*, 2879.

Table II. ^{1}H NMR Spectra of Adducts (δ, $CDCl_3$)

adducts	CH_3	H-1′,8′	H-9′,10′	ArH and others
21	0.93 (s, 6 H)	4.13 (t, 2 H)[a]	6.82 (t, 2 H)	6.9–7.3 (m, 4 H)
22	1.36 (s, 6 H)	4.12 (t, 2 H)[a]	6.65 (t, 2 H)	6.9–7.3 (m, 4 H)
25	0.84 (s, 3 H)	3.47 (m, 2 H)	1.0–1.5 (m, 2 H)[b]	7.0–7.3 (m, 4 H)
	0.97 (s, 3 H)		1.9–2.6 (m, 2 H)[c]	4.55 (s, 1 H, C*H*Cl)
26	1.18 (s, 3 H)	3.51 (m, 2 H)	1.0–1.6 (m, 2 H)[b]	7.0–7.3 (m, 4 H)
	1.47 (s, 3 H)		1.7–2.3 (m, 2 H)[c]	4.13 (s, 1 H, C*H*Cl)
27	1.17 (s, 3 H)	3.15 (m, 1 H)	1.0–1.6 (m, 2 H)[b]	7.0–7.3 (m, 4 H)[d]
	1.28 (s, 3 H)	3.50 (m, 1 H)	1.7–2.2 (m, 2 H)[c]	4.12 (d, 1 H, C*H*Cl)[e]
28	1.00 (s, 6 H)	3.63 (m, 2 H)	1.0–1.5 (m, 2 H)[b]	7.0–7.2 (m, 4 H)
			2.2–2.5 (m, 2 H)[c]	
29	1.42 (s, 6 H)	3.69 (m, 2 H)	1.1–1.7 (m, 2 H)[b]	7.0–7.2 (m, 4 H)
			1.8–2.2 (m, 2 H)[c]	
30a	1.40 (s, 6 H)	4.28 (t, 2 H)[f]	6.85 (t, 2 H)	6.9–7.5 (m, 4 H)
30b	1.23 (s, 6 H)	3.80 (t, 2 H)[f]	6.66 (t, 2 H)	6.8–7.4 (m, 4 H)
				5.5 (br s, 1 H, NH)[g]
31	1.33 (s, 6 H)	3.19 (m, 2 H)	1.0–1.4 (m, 2 H)[b]	6.9–7.3 (m, 4 H)
			1.8–2.2 (m, 2 H)[c]	5.3 (br s, 1 H, NH)[g]
34	1.06 (s, 6 H)	3.49 (m, 2 H)	0.9–1.5 (m, 2 H)[b]	7.0–7.2 (m, 4 H)
			2.2–3.2 (m, 2 H)[c]	6.3 (br s, 1 H, NH)[g]
35	0.98 (s, 6 H)	3.21 (m, 2 H)	1.1–1.6 (m, 2 H)[b]	6.9–7.4 (m, 4 H)
			1.8–2.2 (m, 2 H)[c]	6.6 (br s, 1 H, NH)[g]

[a] $J_{1',10'} = 2.0$ Hz. [b] Endo protons. [c] Exo protons. [d] Plus following signals: δ 1.67 (d, 1 H, $J = 3.0$ Hz, exchangeable, OH) and δ 3.77 (dd, 1 H, $J = 6.0$ and 3.0 Hz, C*H*OH). [e] $J = 6.0$ Hz. [f] $J_{1',10'} = 2.2$ Hz. [g] Exchangeable by D_2O.

Table III. ^{13}C NMR Spectra of Adducts (δ, $CDCl_3$)[a]

adducts	CH_3	C-1	C-2	C-3	C-4	C-1′,8′	C-9′,10′	aromatic C
21	22.22 (q)	194.85 (s)	91.48 (s)	47.89 (s)	103.11 (s)	55.23 (d)	141.05 (d)	122.34 (d), 125.72 (d), 147.03 (s)
22	24.37 (q)	195.83 (s)	91.09 (s)	48.28 (s)	102.40 (s)	55.36 (d)	139.50 (d)	122.08 (d), 125.53 (d), 147.62 (s)
25	21.69 (q)	203.49 (s)	84.15 (s)	37.79 (s)	68.50 (d)	48.83 (d)	25.58[b]	120.64 (d), 121.03 (d), 126.49 (d)
	24.22[b]					48.96 (d)	26.30[b]	144.08 (s), 144.73 (s)
26	19.48 (q)	202.71 (s)	85.25 (s)	38.63 (s)	68.83 (d)	48.31 (d)	25.45[b]	120.05 (d), 120.90 (d), 126.23 (d)
	23.70[b]					48.89 (d)	27.14[b]	126.55 (d), 144.06 (s), 145.25 (s)
27	20.78 (q)	71.55 (d)	69.93 (s)	42.79 (s)	63.50 (d)	45.32 (d)	25.39[b]	120.90 (d), 120.96 (d), 125.77 (d)
	25.19[b]					47.98 (d)	26.43[b]	126.16 (d), 146.03 (s), 146.94 (s)
28	23.26 (q)	197.84 (s)	84.92 (s)	46.78 (s)	91.29 (s)	50.61 (d)	25.86[b]	120.85 (d), 126.76 (d), 144.17 (s)
29	21.77 (q)	197.91 (s)	86.42 (s)	47.50 (s)	91.68 (s)	50.61 (d)	26.51[b]	120.65 (d), 126.57 (d), 144.89 (s)
30b	19.95 (q)		98.95 (s)	52.04 (s)	173.67 (s)	54.12 (d)	138.46 (d)	122.73 (d), 125.46 (d), 147.10 (s)
31	18.58 (q)		83.49 (s)	51.26 (s)	173.48 (s)	47.56 (d)	24.76 (br t)	121.89 (d), 126.44 (d), 145.60 (s)
34	25.13[b]		170.31 (s)	56.62 (s)	79.67 (s)	46.94 (d)	25.65[b]	121.03 (d), 126.16 (d), 145.12 (s)
35	19.61 (q)		81.36 (s)	51.94 (s)	175.70 (s)	46.75 (d)	25.06 (br t)	121.09 (d), 126.36 (d), 144.02 (s)

[a] Downfield from internal tetramethylsilane in $CDCl_3$, and see the structural formula in schemes for numbering of the carbon atoms. [b] Multiplicities were not clear because of signal overlapping.

of phosphorus oxychloride was allowed to react with **1** at room temperature to give 1:1 adducts **20**, **21**, and **22** in 27%, 18%, and 13% yields, respectively (Scheme I). Structural assignments were performed on the basis of elemental analyses and spectroscopic data. The MS spectrum of each adduct showed characteristic peaks for the dichlorinated compound at *m/e* 296 ($M^+ + 4$), 294 ($M^+ + 2$), and 292 (M^+) with relative intensities of 1.1:6.5:10. The IR spectra exhibited a strong carbonyl absorption at 1787–1802 cm^{-1}. The ^{1}H NMR spectrum of **20** displayed signals of aromatic protons at δ 6.9–7.2 (m, 4 H), bridgehead protons at δ 4.17 (t, 2 H, $J = 1.0$ Hz, H-1 and H-8), methine protons at δ 3.76 (dd, 1 H, $J = 6.6$ and 1.5 Hz, H-9) and 2.98 (dd, 1 H, $J = 6.6$ and 1.0 Hz, H-12), and isopropylidene methyl protons at δ 1.65 (s, 3 H) and 1.58 (s, 3 H). The small value of the coupling constants between H-1 and H-12 ($J = 1.0$ Hz) and between H-8 and H-9 ($J = 1.5$ Hz) indicated the exo configuration[36] of adduct **20**.

The symmetric structure of **21** and **22** is particularly evident in their ^{1}H NMR and ^{13}C NMR spectra (see Tables II and III), in which the signals of two methyl groups, H (or C)-1′, -8′, and H (or C)-9′, -10′ appeared in pairs. The four structures of regio- and stereoisomers of the adduct at the exocyclic double bond were conceivable, and no correct structure could be deduced from the above spectroscopic data. Therefore, the structure of **21** was unequivocally established by X-ray diffraction.[37] With the precise structure of **21** in hand, the structure of **22** was determined by comparison of their spectra. In the ^{13}C NMR spectra (see Table III), the chemical shifts of cyclobutanone carbons (C-1–C-4) of **21** and **22** are very similar, suggesting the same addition orientation (regiochemistry) in both adducts. The ^{1}H NMR spectra (see Table II) revealed the dramatic chemical shift difference ($\Delta\delta$ = 0.43 ppm) of the methyl signals due to the different stereochemistry of **21** and **22**. The upfield shift of the methyl signal in **21** is a result of the shielding of the underlying aromatic ring. Furthermore, the Eu(fod)$_3$ shift data strongly support that **22** is a C-2,3 stereoisomer of **21** with the same regiochemical orientation, since the slopes for the olefin protons (α_O) and the benzene protons (α_B) are virtually inverted in both adducts (for **21**, $\alpha_O = 2.8$, $\alpha_B = 0.8$; for **22**, $\alpha_O = 0.8$, $\alpha_B = 1.9$).

The above determined structures were further supported by the following chemical conversions. Treatment of **20** with benzylamine gave the amide **23** in a quantitative yield, while **21** and **22** were recovered unchanged in similar reactions. Furthermore, **20** was converted into the ester **24** in 90% yield by treating it with sodium

(36) Ghosez, L.; Montaigne, R.; Roussel, A.; Vanlierde, H.; Mollet, P. *Tetrahedron* **1971**, *27*, 615.

(37) We are grateful to Dr. Nishikawa, Takeda Pharmaceuticals Co., Ltd., Osaka, and Dr. Kido, Otsuka Pharmaceuticals Co., Ltd., Tokushima, for the structural determination by X-ray diffraction. Space group and cell parameters are as follows. For **21**: space group $P2_1/c$; monoclinic system; $a = 22.47$ Å, $b = 10.31$ Å, $c = 12.42$ Å, $\beta = 99.11°$. For **30b**: space group $P2_12_12_1$; orthorhombic system; $a = 8.65$ Å, $b = 22.20$ Å, $c = 6.10$ Å. The full analytical details will be presented elsewhere.

Scheme II

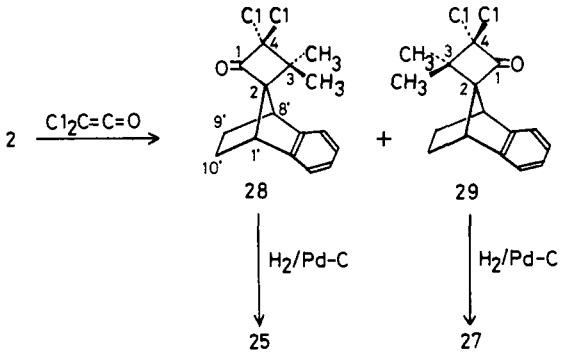

Scheme III

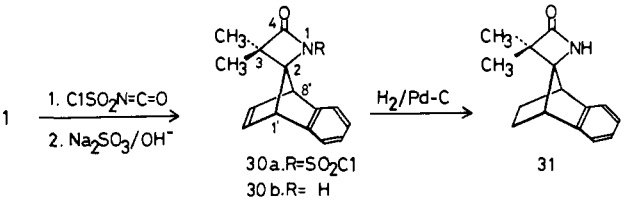

methoxide (Scheme I). These results reflected the increased ring strain of the cyclobutanone ring in **20** compared with that of spiro compounds **21** and **22**.

Catalytic hydrogenation of **21** over palladium on charcoal gave **25** in 70% yield. On the other hand, similar hydrogenation of **22** gave a mixture of **26** and **27** in 37% and 22% yields, respectively (Scheme I). Compound **26** was smoothly converted into the alcohol **27** on further hydrogenation.

Reaction of 2 with Dichloroketene. To estimate the effect of the endocyclic double bond on stereoselectivity in cycloadditions to the exocyclic double bond, we studied the reaction of the dihydro derivative **2**. Dichloroketene generated similarly in situ reacted with **2** at room temperature to give adducts **28** and **29** in 40% and 13% yields, respectively (Scheme II). Elemental analyses and MS spectra showed products to be 1:1 cycloadducts. The detailed analysis of ^1H NMR and ^{13}C NMR spectra (see Tables II and III) indicated these adducts having an element of symmetry to be the stereoisomers with the same regiochemical orientation. The upfield shift ($\Delta\delta$ = 0.42 ppm) of the methyl signal of **28** compared with that of **29** can be attributed to the anisotropic effect of the aromatic ring. The structures of **28** and **29** were further supported by the reductive conversions to **25** and **27**, respectively, which were identified with products obtained from **21** and **22** (Scheme II).

Thus, dichloroketene was found to react with **1** at both endocyclic and exocyclic double bonds. Furthermore, the cycloadditions to the exocyclic double bond of **1** and **2** were stereoselective and regiospecific reactions.

Reaction of 1 with Chlorosulfonyl Isocyanate (CSI). Reaction of **1** with excess chlorosulfonyl isocyanate (CSI) at −78 °C gave a single 1:1 adduct, **30a** in 69% yield. The treatment of **30a** with aqueous sodium bisulfite under basic conditions afforded the corresponding amide **30b** in 95% yield (Scheme III). A detailed structural analysis was performed for **30b**. The IR spectrum exhibited a characteristic band of the β-lactam carbonyl group at 1760 cm^{-1}. The MS spectrum showed a parent ion peak at *m/e* 225 and prominent fragment peaks at *m/e* 182 (7-isopropylidenebenzonorbornadiene) and 156 (8,8-dimethylisobenzofulvene). The ^1H NMR spectrum displayed each single signal for two isopropylidene methyl protons at δ 1.23 (s), two bridgehead protons at δ 3.80 (t), and two olefinic protons at δ 6.60 (t), suggesting the symmetry of molecule. The four isomeric structures for the adduct of the exocyclic double bond are possible. Thus, the unequivocal structure of **30b** was determined by X-ray diffraction.[37] The same reaction of **1** and CSI at room temperature gave also 1:1 adduct **30a** as a sole product. Recently, Paquette and Broadhurst[19] reported the analogous reaction of 7-methylenenorbornadiene (**32**) with CSI at room temperature,

Scheme IV

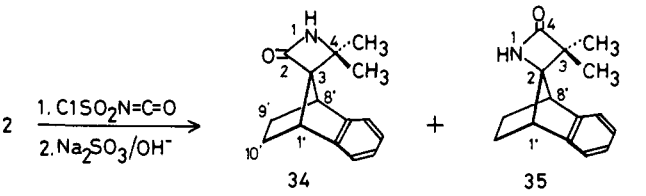

which gave after dechlorosulfonylation, in contrast, a 1:2 adduct **33** in 52% yield (eq 1).

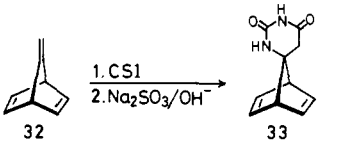

(1)

Catalytic hydrogenation of **30b** gave the dihydro compound **31** (ν_{CO} = 1756 cm^{-1}) in 72% yield. The ^1H and ^{13}C NMR data for these adducts are summarized in Tables II and III.

The above results clearly show that CSI reacts only with the exocyclic double bond of **1** in a stereospecific manner.

Reaction of 2 with CSI. To assess the effect of the nonreacting endocyclic double bond on the stereo- and regioselectivities of CSI addition to **1**, we also studied the reaction of dihydro-derivative **2**. Compound **2** was allowed to react with CSI at −78 °C and the mixture was directly treated with aqueous sodium bisulfite. The chromatographic separation afforded two adducts **34** (90%) and **35** (6.8%) in the order of elution (Scheme IV). None of these was identical with **31** derived from the structurally confirmed **30**. The 1:1 nature of both adducts was apparent from elemental analyses and MS spectra which showed very similar fragmentation patterns: *m/e* 227 (M^+), 184 (7-isopropylidenebenzonorbornene), and 156 (8,8-dimethylisobenzofulvene). In the ^1H NMR spectra (see Table II), the upfield shift (for **34**, $\Delta\delta$ = 0.27 ppm; for **35**, $\Delta\delta$ = 0.35 ppm) of methyl signals relative to those of **31** suggests that methyl groups in these adducts occupy the upside position of the aromatic ring. The IR (KBr) showed a remarkable difference between **34** and **35**. While **35** revealed the "normal" β-lactam carbonyl band at 1753 cm^{-1}, **34** displayed the absorption at 1700 cm^{-1}. The shift to low frequency is apparently due to the intermolecular hydrogen bonding, since this absorption band moves up to 1740 cm^{-1} in a chloroform solution. This suggested the different orientation (regiochemistry) of the amide moiety in **34** compared to that of **31** and **35**. In the ^{13}C NMR spectrum of **34** (Table III), the observed low-field shift of methyl carbon signal (δ 25.13) also supported the above argument. Furthermore, the $Eu(fod)_3$ study in the ^1H NMR of **34** revealed the following shift slopes (α): α(exo H-9′,10′) = 1.0, α(H–N) = 0.7, α(H-1′,8′) = 0.5, α(endo H–H-9′,10′) = 0.4, and α(CH_3) = 0.2. The largest slope for exo H-9′,10′ indicates their proximity to the carbonyl group. Thus, the structure of major product was determined as shown in **34**.

On the other hand, the ^{13}C NMR spectrum of **35** showed very similar β-lactam carbon signals to those of **31** (see Table III), suggesting the same arrangements in the spiro ring. Therefore, the minor product was determined to be the anti stereoisomer of **31** as shown in **35**.

Thus, the CSI addition of **2** also took place in a stereospecific and regioselective manner. However, it should be noted that both stereo- and regioselectivities in these reactions are entirely inverted for **1** and **2**.

Discussion

Periselectivity. The above results show a remarkable periselectivity of **1** in its cycloaddition reactions as shown schematically in Figure 1. The exocyclic double bond is completely inactive in Diels–Alder reactions and 1,3-dipolar cycloadditions.[3,4,6,12] Among several factors, a consideration of its frontier orbitals[11,12] can explain the inactivity of the exocyclic double bond of **1** in the normal (LUMO(1) controlled) Diels–Alder reaction since the LUMO of isopropylidenenorbornadiene system has essentially zero

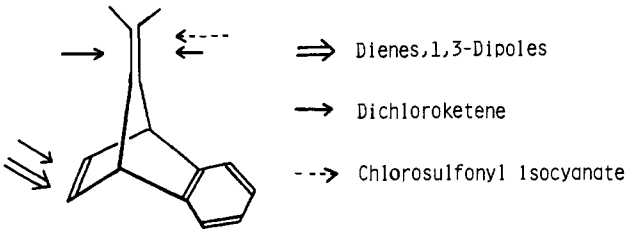

Figure 1. The observed periselectivity in cycloaddition reactions of **1**.

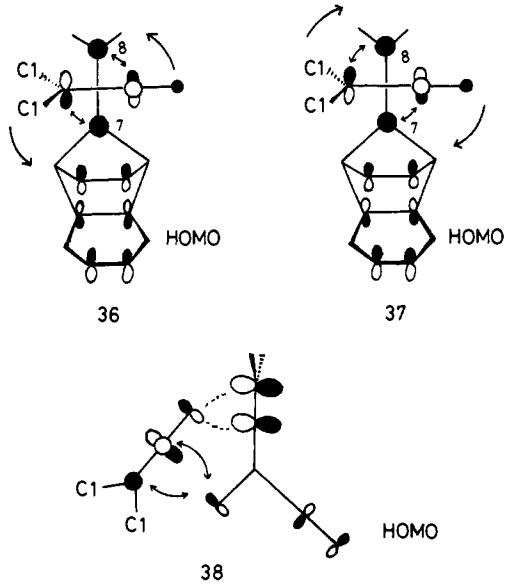

Figure 2. The orthogonal $[{}_{\pi}2_s + {}_{\pi}2_a]$ approach of dichloroketene to **1**.

coefficients at this position.[12,38] In contrast, this external double bond is considered to be the most reactive site in the HOMO-(**1**)-controlled cycloaddition, because the HOMO of **1** has the largest coefficients at the exocyclic double bond.[11] However, the severe steric hindrance and no availability of the stabilizing secondary orbital interaction prevent the approach of addends to the exocyclic double bond. On the other hand, cycloaddition to the strained endocyclic double bond is sterically much favored.

Since all 1,3-dipoles except for diazomethane are considered to react with **1** in dipole LUMO (i.e., HOMO(**1**))-controlled manner,[22,39] the inactivity of this potentially reactive external double bond can be attributed to the steric effect which was also evoked by Hoffmann and Becherer by comparing the frontier orbitals and reactivities with **32**.[41] In contrast, the less hindered internal double bond is activated by the ring strain.[42] These were supported by the diimide reduction which is known to proceed in a concerted manner via the cyclic transition state.[43] The reaction of **1** with a large excess of diimide gave only **2**, and **2** was found to be inert under these reduction conditions.[44] In the reaction of diazomethane which is known as HOMO-controlled dipole,[22] the LUMO(**1**)/HOMO(diazomethane) interaction may

Scheme V

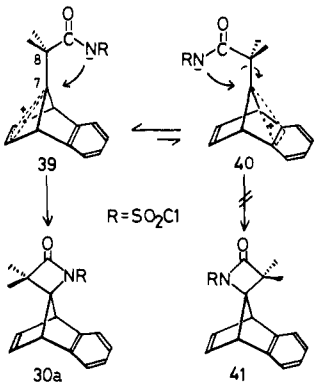

become important. But in this fashion, the exocyclic double bond is electronically inactive as mentioned above.

Thus, *if the steric obstruction could be diminished by some less hindered approaches in the concerted cycloaddition, the reaction would take place at the exocyclic double bond of* **1** *in the HOMO(***1***)-controlled fashion.* Actually, this was realized by the reaction of dichloroketene which is well-known to react with electron-rich olefins in a concerted manner.[46] In this case, the external addition (**21** and **22**, totally 31%) slightly predominated over internal addition (**20**, 27%). An important interaction here is that of HOMO(**1**) and LUMO(ketene). The steric hindrance in the transition state can be substantially reduced by the orthogonal $[{}_{\pi}2_s + {}_{\pi}2_a]$ approach of the ketene to the exocyclic double bond of **1** as depicted in the case of the syn approach, **36** and **37** (Figure 2). Any other skewed transition states like $[{}_{\pi}2_s + {}_{\pi}2_s + {}_{\pi}2_s]$ cycloaddition[47] would be disfavored for steric reasons. Thus, this first example of concerted cycloaddition to the exocyclic double bond of **1** uniquely verified the potential reactivity of this bond. However, the attack to the endocyclic double bond is also favored by both steric factors and stabilizing secondary orbital interactions between the p orbital of the oxygen atom and the exocyclic double bond as shown in **38** (Figure 2). The strain relief cannot be a controlling factor in this case because the four-membered ring is formed in the products.[36] These led to the concurrent formation of **20**–**22**.

In sharp contrast, CSI reacted with **1** exclusively at the most sterically hindered exocyclic double bond.[19,24,25] Since CSI addition proceeds stepwise through the less hindered polarized transition state,[19,41] the electronic factor rather than the steric factor may become predominant. This is consistent with the calculated HOMO electron densities of **1** which show the highest values at the exocyclic double bond.[11,12]

Stereoselectivity and Regioselectivity. Exploration of the stereoselectivity in the electrophilic addition to 7-isoropylidenenorbornene systems is a current subject.[24-27,45] Okada and Mukai have found the parallel relation existing between polarization of the exocyclic double bond and stereoselectivity of singlet oxygen addition.[25,26] Paquette et al. have disclosed that the reaction proceeds via the polarized perepoxide-like transition states and that other electrophilic additions also show similar stereoselectivity.[27] Interestingly, dichloroketene shows the inverted stereoselectivity in the reaction with **1**, whereas CSI has the similar stereochemical tendency. This suggests the different mechanism present for the concerted reaction. In this case, the secondary orbital interaction rather than the orbital distortion[25] seems more important in determining the stereoselectivity. The anti:syn ratio (**21**:**22** = 1.4) appears to be controlled by the extent of the repulsive secondary orbital interactions[25] which both anti and syn approaches would experience with the internal double bond and the aromatic ring, respectively. This was supported by the anti:syn ratio (**28**:**29**

(38) The NLUMO has large coefficients at the exocyclic double bond.[12] Without knowledge of the precise energy level, however, an importance of the NLUMO/HOMO interaction remains unclear at the present stage.

(39) This was also supported by the observation of increased reactivities with these 1,3-dipoles by the order of **1** < 7-azabenzonorbornadiene[30] < 7-oxabenzonorbornadiene.[40]

(40) Sasaki, T.; Kanematsu, K.; Hayakawa, K.; Uchide, M. *J. Chem. Soc., Perkin Trans. 1* **1972**, 2750.

(41) Hoffmann, R. W.; Becherer, J. *Tetrahedron.* **1978**, *34*, 1187.

(42) Huisgen, H. *Angew. Chem., Int. Ed. Engl.* **1963**, *2*, 633.

(43) House, H. O. "Modern Synthetic Reactions", 2nd ed.; W. A. Benjamin: Menlo Park, CA, 1972; pp 248–256.

(44) The inactivity of the tetrasubstituted exocyclic double bond of **1** and **2** is apparently due to the steric hindrance because the disubstituted exocyclic double bond of the related system is reduced by diimide to give syn and anti products.[45]

(45) Hoffmann, R. W.; Havel, N. *Tetrahedron Lett.* **1979**, 4959.

(46) Fleming, I. "Frontier Orbitals and Organic Chemical Reactions"; Wiley: New York, 1976; Chapter 4.

(47) (a) Baldwin, J. E.; Kapecki, J. A. *J. Am. Chem. Soc.* **1970**, *92*, 4868, 4874. (b) Hassner, A.; Cory, R. M.; Sartories, N. *Ibid.* **1976** *98*, 7698.

Scheme VI

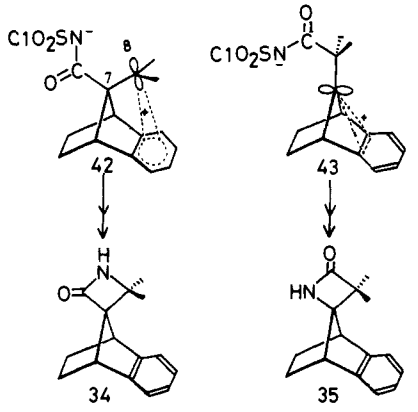

= 3.1) increase in the reaction of **2** in spite of the increased steric hindrance for the anti approach. The similar inverted selectivity was also observed in the diimide reduction of the related systems,[45] suggesting a different mechanism operates for the concerted reaction.

The dichloroketene additions to **1** and **2** are regiospecific. This can be explained in terms of steric hindrance as depicted in Figure 2. The overlap shown in **37** should be favored over **36** because rotation of the ketene in **37** moves the chloro-substituted carbon away from the bulkier norbornene skeleton. This led to the exclusive formation of C-7 carbonylated products. The observation of some regiospecificity for **1** and **2** eliminates all possibilities of ionic mechanism.

It is particularly interesting that stereoselectivity as well as regioselectivity are completely inverted in the reactions of CSI with **1** and **2**. This can be explained in terms of orbital distortion and the stability of the intermediates. In the reaction of **1**, CSI, like other electrophiles,[25,27] will approach the C_7–C_8 bond preferentially from the syn side due to orbital distortion. The initial bond formation at C-8 is thermodynamically preferred since the ionic intermediate **39** can be much stabilized by through space homoconjugation as shown in Scheme V. The anti attack, if present, would also give more stable **39** from the initially formed **40** by C_7–C_8 bond rotation since such a stabilized zwiterionic intermediate is known to have an inordinately long lifetime.[19] In the case of **2**, the anti attack is much favored by the similar orbital distortion caused by the aromatic ring and the observed regioselectivity appears to be a consequence of relative stabilities of intermediates **42** and **43** (Scheme VI). Intermediate **42** leading to **34** seems to be stabilized to a larger extent rather than **43** leading to **35** because of its favorable p orbital angle and distance between the aromatic ring and the cationic center.[48]

Conclusion

Periselectivity of **1** is controlled by both steric and electronic factors. The frontier orbital analysis suggests the most reactive site of **1** in HOMO-controlled reactions to be the external double bond. Therefore, the observed inactivity of the exocyclic double bond in the concerted reactions which require a bulky parallel approach of the addends is mainly a consequence of the steric hindrance. Dichloroketene reacts with **1** in slight preference at the exocyclic double bond because of its less hindered orthogonal approach. In LUMO-controlled reactions, both steric and electronic factors make this bond inactive. In sharp contrast, electrophilic additions which proceed through less hindered polarized transition states ensue predominantly at the electron-rich exocyclic double bond.

Controlling factors of stereo- and regioselectivities in cycloadditions are different for dichloroketene and CSI. The orbital distortion mechanism which has been useful for understanding electrophilic reactions is not important for the concerted reactions, but other factors such as secondary orbital interaction and steric effect become predominant.

Experimental Section

Melting points were measured with a Yanagimoto micromelting point apparatus and are uncorrected. Microanalyses were performed with a Perkin-Elmer 240 elemental analyzer. The ^{1}H NMR spectra were taken at room temperature with a JEOL C-60-HL spectrometer and with a JEOL FX 60 FT NMR spectrometer using tetramethylsilane as an internal standard. The ^{13}C NMR spectra were recorded on a JEOL JNM-FX 60 FT NMR spectrometer at 15.04 MHz in $CDCl_3$. The IR spectra were taken with a JASCO-IRA-1 spectrometer. Mass spectra were obtained with a Hitachi RMS-4 mass spectrometer at 70 eV.

General Procudure for Cycloaddition of 1 with Dienes and 1,3-Dipoles. A solution of **1**[2] and equilmolar dienes **4–6** or 1,3-dipoles **12–15** in an appropriate solvent was heated in a sealed tube or under reflux as listed in Table I. The reaction was monitered by TLC. When the starting materials completely disappeared, heating was stopped and the reaction mixture concentrated under the reduced pressure. The residue was chromatographed on silica gel column by using a mixture of hexane and dichloromethane as an eluant to give the adduct, recrystallization of which from dichloromethane–hexane afforded the analytically pure sample.

Reaction with 1,3-Diphenylbenzofuran (4). The reaction of **1** (182 mg, 1.0 mmol) and **4** (266 mg, 0.99 mmol) gave adduct **7** (429 mg, 95%) as colorless crystals: mp 223–225 °C; IR (KBr) 1600, 1445, 984, 737 cm^{-1}; ^{1}H NMR ($CDCl_3$) δ 1.21 (s, 6 H, CH_3 × 2), 2.53 (s, 2 H, H-2 and H-3), 3.49 (s, 2 H, H-1 and H-4), 6.8–7.8 (m, 18 H, ArH); mass spectrum, (relative intensity) 452 (M^+, 13), 270 (100). Anal. ($C_{34}H_{28}O\cdot{}^1/_2H_2O$): C, H.

Reaction with 1,3-Diphenylphenanthro[9,10-*c*]furan (5). The reaction of **1** (182 mg, 1.0 mmol) and **5**[49] (370 mg, 1.0 mmol) gave adduct **8** (453 mg, 82%) as colorless crystals: mp >300 °C; IR (KBr) 1450, 1010, 750 cm^{-1}; ^{1}H NMR ($CDCl_3$) δ 0.93 (s, 6 H, CH_3 × 2), 2.73 (s, 2 H, H-2 and H-3), 4.18 (s, 2 H, H-1 and H-4), 6.8–8.7 (m, 22 H, ArH); mass spectrum, *m/e* 552 (M^+). Anal. ($C_{42}H_{32}O\cdot{}^1/_2H_2O$): C, H.

Reaction with *o*-Chloranil (6). The reaction of **1** (546 mg, 3.0 mmol) and **6** (738 mg, 3.0 mmol) gave adduct **9** (231 mg, 18%): mp 258–259 °C; IR (KBr) 1565, 1430, 1057, 1000 cm^{-1}; ^{1}H NMR ($CDCl_3$) δ 1.44 (s, 6 H, CH_3 × 2), 4.07 (s, 2 H, H-1 and H-4), 4.62 (s, 2 H, H-2 and H-3), 7.2 (m, 4 H, ArH). Anal. ($C_{20}H_{14}Cl_4O_2$): C, H.

Reaction with 1-Methylpyridinium-3-olate (12). The reaction of **1** (182 mg, 1.0 mmol) and **12**[50] (120 mg, 1.1 mmol) gave adduct **16** (29 mg, 10%) as yellow prisms: mp 168–170 °C; IR (KBr) 1660, 1370, 1157, 700 cm^{-1}; ^{1}H NMR ($CDCl_3$) δ 1.61 (s, 6 H, CH_3 × 2), 2.01 (d, 1 H, J = 7.5 Hz, H-2), 2.20 (d, 1 H, J = 7.5 Hz, H-3), 2.39 (s, 3 H, NCH_3), 3.37 (s, 1 H, H-1′), 3.59 (d, 1 H, J = 4.6 Hz, H-5′), 3.74 (s, 1 H, H-1), 3.83 (s, 1 H, H-4), 5.83 (dd, 1 H, J = 9.9 and 1.0 Hz, H-3′), 6.87 (dd, 1 H, J = 9.9 and 4.6 Hz, H-4′), 7.0–7.3 (m, 4 H, ArH). Anal. ($C_{20}H_{21}NO$): C, H, N.

Reaction with *C*-Phenyl-*N*-benzylnitrone (13). The reaction of **1** (182 mg, 1.0 mmol) and **13** (230 mg, 1.09 mmol) gave adduct **17** (296 mg, 75%) as colorless crystals: mp 154–156 °C; IR (KBr) 1455, 750 cm^{-1}; ^{1}H NMR ($CDCl_3$) δ 1.67 (s, 3 H, CH_3), 1.71 (s, 3 H, CH_3), 2.64 (t, 1 H, J = 7.2 Hz, H-2), 3.26 (d, 1 H, J = 7.2 Hz, C*H*Ph), 3.65 (s, 2 H, H-1 and H-4), 3.84 (s, 2 H, CH_2Ph), 4.28 (d, 1 H, J = 7.2 Hz, H-3), 6.9–7.5 (m, 14 H, ArH). Anal. ($C_{28}H_{27}NO$): C, H, N.

Reaction with Phenylglyoxylonitrile Oxide (14). The reaction of **1** (182 mg, 1.0 mmol) and **14**[51] prepared in situ from phenylglyoxylohydroxamic acid chloride (185 mg, 1.0 mmol) and triethylamine (1.0 mmol) in dry ether gave adduct **18** (297 mg, 90%): mp 178–180 °C; IR (KBr) 1643, 1373, 1255, 920 cm^{-1}; ^{1}H NMR ($CDCl_3$) δ 1.51 (s, 3 H, CH_3), 1.73 (s, 3 H, CH_3), 3.92 (d, 1 H, J = 7.5 Hz, H-2), 4.21 (s, 1 H, H-1), 4.25 (s, 1 H, H-4), 4.96 (d, 1 H, J = 7.5 Hz, H-3), 7.0–7.7 (m, 7 H, ArH), 8.0–8.25 (m, 2 H, ArH). Anal. ($C_{22}H_{19}NO_2$): C, H, N.

Reaction with Diazomethane (15). The reaction of **1** (126 mg, 0.7 mmol) and an excess of **15** gave adduct **19** (124 mg, 80%) as colorless crystals: mp 110–112 °C; IR (KBr) 1455, 742 cm^{-1}; ^{1}H NMR ($CDCl_3$) 1.54 (s, 3 H, CH_3), 1.60 (s, 3 H, CH_3), 2.16 (m, 1 H, H-2), 3.54 (s, 1 H, H-1), 4.14 (m, 2 H, CH_2), 4.35 (s, 1 H, H-4), 4.94 (br d, 1 H, J = 6.2 Hz, H-3), 7.0–7.4 (m, 4 H, ArH). Anal. ($C_{15}H_{16}N_2$): C, H, N.

Reaction of 1 with Dichloroketene. The cycloaddition of dichloroketene to olefins **1** and **2** was carried out according to Hassner's procedure.[35] To a stirred mixture containing **1** (874 mg, 4.8 mmol), activated

(48) The long-range stabilization by aryl π participation has been recognized in the solvolytic work: Haslanger, M.; Zawacky, S.; Lawton, R. G. *J. Org. Chem.* 1976, *41*, 1807 and references cited therein.

(49) Basselier, J. J.; Roux, J. P.; Caumartin, F.; Chertone, J. C. *Bull. Soc. Chim. Fr.* **1974**, 2950.

(50) Katritzky, A. R.; Takeuchi, Y. *J. Chem. Soc. C* **1971**, 874.

(51) For a recent review, see: Grundmann, C.; Grünanger, P. "The Nitrile Oxides"; Spring-Verlag: West Berlin, 1971.

zinc dust (345 mg, 5.3 mmol) and dry ether (10 mL) were added slowly a solution of trichloroacetyl chloride (0.55 mL, 915 mg, 5.0 mmol) and phosphorus oxychloride (0.46 mL, 765 mg, 5.0 mmol) in dry ether (5 mL) under argon over 0.5 h. After the stirring was continued for 2 days at room temperature, the reaction mixture was then filtered through a pad of Celite and the unreacted zinc washed with 25 mL of ether. The etheral solution was concentrated in vacuo to ca. 25% of its original volume, and an equal volume of pentane was added. The solution was stirred for a few minutes to precipitate the zinc salts and decanted. The organic layer was washed successively with water and a cold saturated $NaHCO_3$ solution and dried over $MgSO_4$. After removal of the solvent, the resulting residue was chromotographed on a silica gel column by using hexane–dichloromethane (20:1). The first fractions gave adduct **20** (380 mg, 27%) as colorless needles: mp 110–120 °C (hexane–dichloromethane); IR (KBr) 1802, 1440, 1372, 1153, 1009, 746, 736 cm^{-1}; ^1H NMR ($CDCl_3$) δ 1.58 (s, 3 H, CH_3), 1.65 (s, 3 H, CH_3), 2.98 (dd, 1 H, J = 6.6 and 1.0 Hz, H-12), 3.76 (dd, 1 H, J = 6.6 and 1.5 Hz, H-9), 4.17 (t, 2 H, J = 1.0 Hz, H-1 and H-8), 6.9–7.2 (m, 4 H, ArH); ^{13}C NMR ($CDCl_3$) δ 19.95 (q, Me), 21.05 (q, Me), 45.74 (d, C-1), 47.11 (d, C-8), 55.68 (d, C-12), 65.88 (d, C-9), 82.84 (s, C-11), 119.74 (s, C-14), 140.47 (s, C-13), 121.04 (d), 121.37 (d), 126.57 (d), 126.70 (d), 144.82 (s), 145.60 (s) (aromatic-C), 192.91 (s, C-10); mass spectrum, m/e (relative intensity) 296 (M^+ + 4, 0.3), 294 (M^+ + 2, 1.2), 292 (M^+, 1.9), 251 (5), 249 (7), 179 (9.5), 178 (10), 156 (100), 141 (16), 128 (5.6), 115 (8.6). Anal. ($C_{16}H_{14}Cl_2O$): C, H.

The second fractions gave adduct **21** (252 mg, 18%) as colorless needles: mp 127–129 °C (hexane–dichloromethane); IR (KBr) 1787, 1445, 1170, 825, 741, 710, 690 cm^{-1}; mass spectrum, m/e (relative intensity) 296 (M^+ + 4, 2.4), 294 (M^+ + 2, 15), 292 (M^+, 23), 231 (42.5), 229 (43.5), 193 (36), 182 (18), 178 (43.5), 168 (32.5), 140 (100), 115 (25). ^1H NMR and ^{13}C NMR data are summarized in Tables II and III. In a Eu(fod)$_3$ study, the slopes for the olefinic (H-9′,10′), bridgehead (H-1′,8′), aromatic, and methyl protons were 2.8, 1.8, 0.8, and 1.4, respectively. A plot of the shifts vs. molar equiv of shift reagent is linear to 0.03–0.15 molar equiv and then levels off. Anal. ($C_{16}H_{14}Cl_2O$): C, H.

The third fractions gave adduct **22** (182 mg, 13%) as colorless needles: mp 133–134 °C (hexane–dichloromethane); IR (KBr) 1795, 1457, 1173, 807, 796, 737 cm^{-1}; mass spectrum, m/e (relative intensity) 296 (M^+ + 4, 1.1), 294 (M^+ + 2, 6.6), 292 (M^+, 9.5), 257 (21), 229 (37), 194 (24), 140 (100), 128 (55). ^1H NMR and ^{13}C NMR data are summarized in Tables II and III. The relative Eu(fod)$_3$ slopes for the olefinic (H-9′,10′), bridgehead (H-1′,8′), aromatic, and methyl protons were 0.8, 1.5, 1.9, and 0.6, respectively. Anal. ($C_{16}H_{14}Cl_2O \cdot {}^1/_3H_2O$): C, H.

The reaction was repeated three times under the same conditions in a 2.0-mmol scale and the product distributions determined by ^1H NMR analysis were the same as above within experimental errors.

Reaction of 20 with Benzylamine. Adduct **20** (70 mg, 0.24 mmol) in dry ether (0.4 mL) was treated with benzylamine (60 mg, 0.56 mmol) at room temperature. After 0.5 h the precipitated crystals were collected and recrystallized from ethanol to give **23** (90 mg, 94%) as needles: mp 145–147 °C; IR (KBr) 3225, 1632, 1550, 1241, 743 cm^{-1}; ^1H NMR ($CDCl_3$) δ 1.65 (s, 3 H, CH_3), 1.70 (s, 3 H, CH_3), 2.30 (d, 1 H, J = 8.5 Hz, H-2), 2.56 (t, 1 H, J = 9.0 Hz, H-3), 3.85 (d, 1 H, J = 1.7 Hz, H-1 or H-4), 4.16 (d, 1 H, J = 1.7 Hz, H-1 or H-4), 4.38 (d, 2 H, J = 5.4 Hz, CH_2Ph), 5.82 (br s, 1 H, exchangeable, NH), 6.11 (d, 1 H, J = 9.0 Hz, CHCl$_2$), 6.9–7.4 (m, 9 H, ArH). Anal. ($C_{23}H_{23}Cl_2NO$): C, H, N.

Treatment of 20 with Sodium Methoxide. A solution of sodium methoxide (22 mg, 0.4 mmol) in methanol (0.6 mL) was added dropwise to a cooled (−15 °C) solution of **20** (62 mg, 0.21 mmol) in 1 mL of ether–methanol (1:1). The resulting solution was stirred at −5 °C for 2 h. After neutralization with successive addition of 5% HCl and aqueous $NaHCO_3$ solution, the mixture was concentrated in vacuo and extracted with ether. Evaporation of the ethereal solution left **24** (62 mg, 90%) which was recrystallized from methanol: mp 112–114 °C; IR (KBr) 1722, 1437, 1360, 1158 cm^{-1}; ^1H NMR ($CDCl_3$) δ 1.67 (s, 3 H, CH_3), 1.71 (s, 3 H, CH_3), 2.65 (m, 2 H, H-2 and H-3), 3.68 (s, 3 H, CH_3), 3.88 (d, 1 H, J = 1.5 Hz, H-1 or H-4), 4.14 (d, 1 H, J = 1.5 Hz, H-1 or H-4), 5.91 (dd, 1 H, J = 7.0 and 3.0 Hz, CHCl$_2$), 7.0–7.3 (m, 4 H, ArH). Anal. ($C_{17}H_{18}Cl_2O_2$): C, H.

Hydrogenation of 21. A solution of **21** (48 mg, 0.16 mmol) in 95% ethanol (1.5 ml) was hydrogenated over 10% Pd/C (68 mg) under atmospheric pressure of hydrogen to give **25** (29 mg, 70%) as colorless needles: mp 75–78 °C; IR (KBr) 1780, 1470, 1380, 1280, 765 cm^{-1}. ^1H NMR and ^{13}C NMR data are summarized in Tables II and III.

Anal. ($C_{16}H_{17}ClO$): C, H.

Hydrogenation of 22. A solution of **22** (60 mg, 0.21 mmol) in 95% ethanol (1.5 mL) was hydrogenated over 10% Pd/C (50 mg) under atmospheric pressure of hydrogen. The reaction mixture was chromatographed on silica gel by using hexane–dichloromethane to give **26** (20 mg, 37%) and **27** (12 mg, 22%) in the order of elution.

The ketone **26**: mp 94–96 °C; IR (KBr) 1770, 1458, 1257, 1080, 790, 742 cm^{-1}. ^1H NMR and ^{13}C NMR data are summarized in Tables II and III.

Anal. ($C_{16}H_{17}ClO$): C, H.

The alcohol **27**: mp 153–155 °C; IR (KBr) 3470, 1453, 1440, 1100, 743 cm^{-1}. ^1H NMR and ^{13}C NMR data are summarized in Tables II and III.

Anal. ($C_{16}H_{19}ClO$): C, H.

The conversion of **26** into **27** was observed on the hydrogenation under the same conditions as above.

Reaction of 2 with Dichloroketene. Following the procedure described above, **2** (883 mg, 4.8 mmol) and activated zinc (345 mg, 5.3 mmol) in dry ether (10 mL) were treated with a solution of trichloroacetyl chloride (0.55 mL, 915 mg, 5.0 mmol) and phosphorus oxychloride (0.46 mL, 765 mg, 5.0 mmol) in dry ether (5 mL). The reaction mixture was stirred for 2 days at room temperature. Similar workup followed by chromatography on silica gel with hexane–dichloromethane gave adducts **28** (565 mg, 40%) and **29** (183 mg, 13%) in the order of elution.

Adduct **28**: mp 101–103 °C (hexane–dichloromethane): IR (KBr) 1790, 1465, 1203, 838, 748 cm^{-1}; mass spectrum, m/e (relative intensity) 298 (M^+ + 4, 1.7), 296 (M^+ + 2, 10.8), 294 (M^+, 16.5), 231 (35), 203 (37), 195 (55), 169 (90), 165 (65), 141 (100), 129 (86). ^1H NMR and ^{13}C NMR data are summarized in Tables II and III.

Anal. ($C_{16}H_{16}Cl_2O$): C, H.

Adduct **29**: mp 168–170 °C (hexane–dichloromethane); IR (KBr) 1786, 1459, 1210, 1079, 752 cm^{-1}; mass spectrum, m/e (relative intensity) 298 (M^+ + 4, 0.5), 296 (M^+ + 2, 3.5), 294 (M^+, 5.4), 171 (65), 142 (78), 128 (100). ^1H NMR and ^{13}C NMR data are summarized in Tables II and III.

Anal. ($C_{16}H_{16}Cl_2O$): C, H.

Hydrogenation of 28. A solution of **28** (52 mg, 0.18 mmol) in 95% ethanol (1.5 mL) was hydrogenated over 10% Pd/C (40 mg) under atmospheric pressure of hydrogen to give **25** (30 mg, 65%) which was identical with the product obtained from **21** in all aspects.

Hydrogenation of 29. Adduct **29** (25 mg, 0.085 mmol) was similarly hydrogenated to give **27** (16 mg, 72%). All the physical data were identical with those of **27** obtained from **22** and **26**.

Reaction of 1 with Chlorosulfonyl Isocyanate (CSI). To a stirred and cooled (−78 °C) solution of **1** (546 mg, 3.0 mmol) in dry ether (15 mL) was added slowly CSI (0.46 mL, 5.3 mmol) in dry ether (15 mL) under argon over 0.5 h. After the stirring was continued for 8 h at −78 °C, the mixture was warmed to room temperature and then diluted with hexane to precipitate **30a** (670 mg, 69%) as colorless crystals: mp 143–145 °C; IR (KBr) 1805, 1400, 1180, 1172, 1102, 1056, 805, 740, 685 cm^{-1}. ^1H NMR data are summarized in Table II.

Anal. ($C_{15}H_{14}NO_3SCl$): C, H, N.

Dechlorosulfonylation of 30a. A mixture of **30a** (670 mg, 2.1 mmol), ether (50 mL), and 20% aqueous Na_2SO_3 (40 mL) was stirred at room temperature for 1 day, during which time the aqueous phase was kept between pH 8 and 9 by occasional addition of 10% aqueous KOH. The organic layer was separated, and the aqueous layer was extracted with ether (4 × 20 mL). The combined organic layer was dried ($MgSO_4$) and evaporated to afford **30b** (445 mg, 95%) as colorless crystals: mp 226–227 °C (hexane–dichloromethane); IR (KBr) 3200, 1760, 1712, 1455, 1367, 1290, 1225, 1040, 748, 687 cm^{-1}; mass spectrum, m/e (relative intensity) 225 (M^+, 26), 210 (12), 197 (20), 182 (47), 167 (68), 156 (90), 155 (84), 128 (90), 83 (30), 69 (100). ^1H NMR and ^{13}C NMR data are summarized in Tables II and III.

Anal. ($C_{15}H_{15}NO$): C, H, N.

Hydrogenation of 30b. A solution of **30b** (76 mg, 0.34 mmol) in 95% ethanol (1.5 mmol) was hydrogenated over 10% Pd/C (60 mg) under atmospheric pressure of hydrogen to give **31** (56 mg, 72%) as colorless crystals: mp 245 °C dec; IR (KBr) 3175, 1756, 1455, 1397, 1372, 1050, 748 cm^{-1}. ^1H NMR and ^{13}C NMR data are summarized in Tables II and III.

Anal. ($C_{15}H_{17}NO$): C, H, N.

Reaction of 2 with CSI. A mixture of **2** (492 mg, 2.7 mmol) and CSI (0.4 mL, 4.5 mmol) in dry ether (50 mL) was stirred at −78 °C. After the dechlorosulfonylation as outlined above, chromatography of the reaction mixture on silica gel by using ether–hexane gave adducts **34** (791 mg, 90%) and **35** (60 mg, 6.8%) in the order of elution.

Adduct **34**: mp 242–244 °C; IR (KBr) 3270, 1700, 1370, 1275, 760 cm^{-1}; IR ($CHCl_3$) 3410, 1740, 1460, 1340 cm^{-1}; mass spectrum, m/s (relative intensity) 227 (M^+, 22), 184 (42), 169 (58), 156 (100). ^1H NMR and ^{13}C NMR data are summarized in Tables II and III. In a Eu(fod)$_3$ study, the slopes for exo H-9′,10′, H-N, H-1′,8′, endo H-9′,10′, and CH_3 protons were 1.0, 0.7, 0.5, 0.4, and 0.2, respectively. The shift plot was linear up to 0.3 molar equiv of shift reagent per mole of **34**.

Anal. ($C_{15}H_{17}NO$): C, H, N.

Adduct **35**: mp 223-225 °C; IR (KBr) 1753, 1702, 1460, 1250, 1120, 1050, 745 cm^{-1}; mass spectrum, *m/e* (relative intensity) 227 (M^+, 10), 184 (42), 169 (53), 156 (100). ^1H NMR and ^{13}C NMR data are summarized in Tables II and III.

Anal. ($C_{15}H_{17}NO$): C, H, N.

Diimide Reduction of 1 and 2. To a solution of **1** (182 mg, 1 mmol) in aqueous methanol (10 mL) were added 1% aqueous cupric acetate solution (0.2 ml) and 64% hydrazine (1.2 mL, 24.2 mmol). After being stirred for 20 h at room temperature under bubbling air, water (50 mL) was added and the precipitate was collected by filtration to give **2** (184 mg, 100%) as colorless solid, mp 91-92 °C (lit.[2] mp 90.5-91.5 °C).

Compound **2** (92 mg, 0.5 mmol) was treated with 64% hydrazine (0.6 mL, 12.1 mmol) for 10 h under the same conditions. The workup afforded the unchanged **2** (85 mg).

Acknowledgment. We are indebted to Dr. G. L'abbé for helpful discussions in ^{13}C NMR analyses of β-lactams. We also thank Mr. E. Wakabayashi for the experimental assistance.

Catalysis of the Methoxyaminolysis of Phenyl Acetate by a Preassociation Mechanism with a Solvent Isotope Effect Maximum[1]

Michael M. Cox and William P. Jencks*

Contribution No. 1340 from the Graduate Department of Biochemistry, Brandeis University, Waltham, Massachusetts 02254. *Received July 7, 1980*

Abstract: General-acid catalysis of the reaction of methoxyamine with phenyl acetate by the proton, carboxylic acids, and ammonium ions follows a nonlinear Brønsted curve. This curve agrees quantitatively with the behavior expected for the enforced preassociation mechanism of catalysis that was predicted for this reaction. The stronger acids, including the proton, follow a Brønsted slope of $\alpha = 0.16$ that represents rate-limiting amine attack assisted by hydrogen bonding, weaker acids react with partially rate-limiting proton transfer to the addition intermediate $T^{\pm}$, and the weakest acids follow a steeper Brønsted slope approaching $\alpha = 1.0$ that represents rate-limiting separation of the conjugate base from the protonated intermediate T^+. There is no decrease in the rate constant for catalysis by chloroacetic acid with increasing viscosity in water-glycerol mixtures; a decrease is observed for the reaction of methylamine with *p*-tolyl acetate catalyzed by acetate buffers, which is believed to proceed by a diffusion-controlled trapping mechanism. A sharp maximum in the solvent isotope effect at $pK_{HA} = 6.8$ confirms the kinetically significant proton-transfer step in the intermediate region near $\Delta pK = 0$. The decrease with stronger acids represents a decrease in the isotope effect for this proton-transfer step, which is largely rate limiting for acids of $pK_a = 4$-7, but the decrease with weaker acids can be explained by the change to rate-limiting diffusional separation of T^+ and A^-. Two explanations are offered for the decreased isotope effect with increasing acid strength. (1) There is a sharp change to an asymmetric structure of the transition state for the very rapid proton-transfer step, as suggested by Melander and Westheimer. (2) There is a shift to a rate-limiting change in solvation that occurs immediately either before or after the proton-transfer step with stronger acids. It is possible to fit the observed Brønsted curve and isotope effect maximum with calculated rate constants that are based on a rate law and estimated rate constants for the steps of the latter mechanism.

We describe here evidence that the reaction of methoxyamine with phenyl acetate proceeds through a tetrahedral addition intermediate, T^+, which is sufficiently unstable that the reaction is forced to proceed through a preassociation mechanism in which the amine, the ester, and a molecule of catalyzing acid come together in an encounter complex before the N-C bond is formed. We also discuss possible explanations for the sharp solvent isotope effect maximum with changing pK_a of the catalyzing acid for this reaction, including a mechanism that involves kinetically significant solvent reorientation steps. Some of this work has been reported in preliminary communications.[2,3]

The attack of methylamine on *p*-tolyl acetate gives an addition intermediate, $T^{\pm}$, that reverts to reactants with a rate constant of $k_{-1} \approx 3 \times 10^9\ s^{-1}$ if it is not trapped by protonation after encounter with a molecule of buffer acid or base (eq 1). These conclusions are based on typical "Eigen curves" for catalysis of ester formation and on a leveling of the product ratio as the acid concentration is increased when the addition intermediate is generated by addition of water to the corresponding imidate.[4]

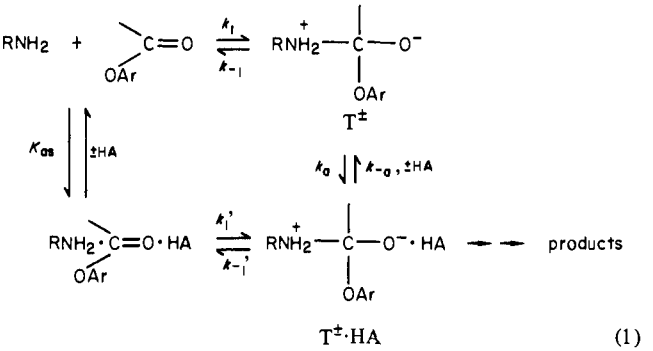

(1)

General-acid catalysis of the aminolysis reaction involves trapping of the intermediate by encounter of $T^{\pm}$ with a buffer acid to form the complex $T^{\pm}$·HA (k_a, eq 1), so that it can undergo proton transfer and go on to products rather than revert to reactants (k_{-1} or k_{-1}', eq 1).

The complex $T^{\pm}$·HA may also be formed through an alternative route by a preassociation mechanism. In this mechanism the reactants and catalyst come together in an encounter complex prior to addition of the amine, as shown in the lower path through K_{as}

(1) Supported by grants from the National Science Foundation (Grant BG-31740) and the National Institutes of Health (Grants GM20888 and GM20168). M.M.C. was supported by a training grant from the National Institutes of Health (Grant 5-T01-GM00212).

(2) Cox, M. M.; Jencks, W. P. *J. Am. Chem. Soc.* **1978**, *100*, 5956-5957.

(3) Cox, M. M.; Jencks, W. P. *Fed. Proc., Fed. Am. Soc. Exp. Biol.* **1979**, *38*, 473.

(4) Satterthwait, A. C.; Jencks, W. P. *J. Am. Chem. Soc.* **1974**, *96*, 7031-7044.

0002-7863/81/1503-572$01.00/0